

A new method for determining OBS positions for crustal structure studies, using airgun shots and precise bathymetric data

Atsushi Oshida^{1,4} Ryuji Kubota¹ Eiichiro Nishiyama¹ Jun Ando¹ Junzo Kasahara²
Azusa Nishizawa³ Kentaro Kaneda³

¹Kawasaki Geological Engineering Co. Ltd., 2-11-15 Mita, Minato-ku, Tokyo 108-8337, Japan.

²Japan Continental Shelf Survey Co. Ltd., 1-11-2 Kyobashi, Chuo-ku, Tokyo 104-0031, Japan.

³Hydrographic and Oceanographic Department, Japan Coast Guard, 5-3-1 Tsukiji, Chuo-ku, Tokyo 104-0045, Japan.

⁴Corresponding author. Email: oshidaa@kge.co.jp

Abstract. Ocean-bottom seismometer (OBS) positions are one of the key parameters in an OBS-airgun seismic survey for crustal structure study. To improve the quality of these parameters, we have developed a new method of determining OBS positions, using airgun shot data and bathymetric data in addition to available distance measurements by acoustic transponders. The traveltimes of direct water waves emitted by airgun shots and recorded by OBSs are used as important information for determining OBS locations, in cases where there are few acoustic transponder data (<3 sites).

The new method consists of two steps. A global search is performed as the first step, to find nodes of the bathymetric grid that are the closest to explaining the observed direct water-wave traveltimes from airgun shots, and acoustic ranging using a transponder system. The use of precise 2D bathymetric data is most important if the bottom topography near the OBS is extremely rough. The locations of the nodes obtained by the first step are used as initial values for the second step, to avoid falling into local convergence minima. In the second step, a non-linear inverse method is executed.

If the OBS internal clock shows large drift, a secondary correction for the OBS internal clock is obtained, as well as the OBS location, as final results by this method. We discuss the error and the influence of each measurement used in the determination of OBS location.

Key words: OBS, crustal structure, OBS position, airgun, bathymetric grid data, acoustic transponder.

Introduction

Crustal structure studies have recently become of great importance in understanding the nature of the ocean-continent transition in oceanic regions, and of earthquake generation mechanisms on land and at sea. In crustal structure studies in oceanic regions, ocean bottom seismometers (OBSs) and airguns are powerful tools for estimating seismic velocities in the crust and the mantle. The determination of OBS locations is a key step in crustal structure studies. The most usual method of determining OBS locations is to use distance measurements between an OBS and a ship by acoustic transponders. In order to obtain the OBS locations precisely, however, it is necessary to use several transponder measurements, with high signal-to-noise ratio signals at more than three appropriate ship positions, and it is sometimes difficult to achieve this under the limited availability of ship time. Nakamura et al. (1987) and Shiobara et al. (1997) proposed to use airguns in addition to transponder measurements for determination of OBS positions. However, OBS location strongly depends on the accuracy of the internal clock of the OBS, the water depth around the OBS, accuracy of transponder measurements, and sound speed in seawater. By considering those effects, we have developed a new method to determine the OBS location by use of precise bathymetric grid data and the direct water-wave traveltimes of the airgun shots recorded by the OBSs, in addition to the acoustic ranging between the OBS and the survey ship.

The procedure of the new method is separated into two steps: a global search for candidate locations using precise bathymetric

data, and non-linear inversion using all available data (Figure 1). The non-linear inverse method is applied to improve the initial estimate of the OBS location from the global search. This procedure enables us to avoid local minima of the convergence during the non-linear inversion step. Our method also gives a secondary correction term for the OBS internal clock. This new method has been successfully used in the continental shelf surveys in Japan, as a pre-processor in the integrated method of refracted-wide angle reflection seismology in oceanic regions (Kasahara et al., 2007).

Method

To determine OBS positions we use several measurements, listed in Table 1. Taking into consideration the accuracy of each measurement, we find an optimum OBS location.

Input data

We use the following inputs for the global search method (see Table 1):

- 1) a precise bathymetric grid data,
- 2) an OBS deployment location as an initial value,
- 3) shot times of airguns and the differential GPS (DGPS)/GPS locations of airgun shots,
- 4) direct water-wave arrival times of airgun shots,
- 5) acoustic ranging between an OBS and GPS ship positions, and
- 6) an average sound-speed of seawater around the survey area.

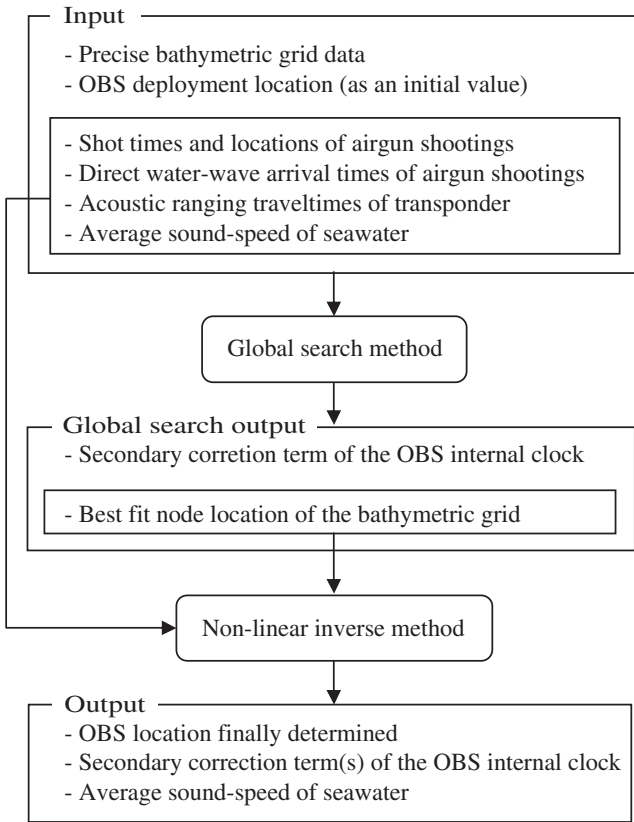


Fig. 1. Processing flow scheme for the global search and non-linear inversion methods.

If we independently know the average sound-speed of seawater from XBT (Expendable BathyThermograph) or XCTD (Expendable Conductivity, Temperature, and Depth profiler) measurements, that is used as an input parameter. The observations in 3)–6) in the above list are also used for the non-linear inversion method (Figures 1 and 2).

Each direct water-wave traveltime $t_{\text{shot_obs}}(k)$, to the OBS from the k -th airgun shot position $(x_k^{\text{shot}}, y_k^{\text{shot}})$, is obtained by

$$t_{\text{shot_obs}}(k) = t_{\text{shot_pick}}(k) - t_0(k) + dt(k), \quad (1)$$

where $t_{\text{shot_pick}}(k)$ is the arrival time of a direct water-wave picked on the seismic record, and $t_0(k)$ is the shot time. In this equation, $dt(k)$ is the estimated time correction for the k -th shot.

The direct water-wave traveltimes of the airgun shots are picked on the seismic record sections for the hydrophone channel or vertical geophone channel of the assigned OBS (Figure 3). The initial correction term for the OBS internal clock, $dt(k)$, is obtained by linear interpolation between dt_{before} just before deployment and dt_{after} just after recovering of the OBS. The seismic record section of the OBS is edited from the raw data using the dt -corrected OBS internal clock times. We think that a secondary correction term for the OBS internal clock can be necessary if the time correction is not accurate enough, and try to separate it in the global search and the non-linear inverse methods.

The precise bathymetric grid data around the OBS deployment location, z_{ij} , at each position (x_{ij}, y_{ij}) are usually determined from the multi-beam echo-sounder data. This grid has a node interval of 0.0005 degrees (~ 55 m) in both latitudinal and longitudinal directions. The grid area for the global

Table 1. Parameters used for OBS positioning and their errors.

| | Parameter | Error | Estimated measurement errors | Units | Methods | Comments |
|--------------------------------|--|-------------------------------|--------------------------------------|-------------|------------------------------|----------------|
| Air gun shots | | | | | | |
| Shot number | $k(x,y)$ | | | | Airgun | |
| Shot time | $t_0(k)$ | ϵ_t | $\sim 10 \mu\text{sec}$ | D:H:M:S | GPS clock | |
| Shot position | $x_k^{\text{shot}}, y_k^{\text{shot}}$ | $\epsilon_{\text{shot_pos}}$ | A few metres | deg:min:sec | DGPS/GPS | |
| Shot depth | z_k^{shot} | | A few metres | metre | | |
| Estimated time correction | $dt(k)$ | ϵ_{dt} | $\sim 10\text{--}20$ msec by clock | msec | | |
| Arrival time picking | $t_{\text{shot_pick}}(k)$ | ϵ_{pick} | ~ 10 msec | D:H:M:S | OBS | |
| Traveltime | $t_{\text{shot_obs}}(k)$ | $\epsilon_t + \epsilon_{dt}$ | | | $t_{\text{read}} - t_0 + dt$ | |
| Transponder* | | | | | | |
| Ship position | $x_l^{\text{trans}}, y_l^{\text{trans}}$ | $\epsilon_{\text{ship_pos}}$ | A few 10 m | deg:min:sec | GPS/DGPS | |
| Transponder depth | z_1^{trans} | | A few metres | metres | | |
| Traveltime | $t_{\text{trans_obs}}(I)$ | ϵ_t | < 1 msec | sec | Correlation | At calm sea |
| Distance | Δ_l | ϵ_{Δ} | Unstable values $< 1\text{--}2$ m | metre | | At rough sea |
| Average sound-speed | | | | | | |
| | v_w | ϵ_v | ~ 10 m/sec | m/sec | | |
| Bathymetry** | | | | | | |
| Position | x_{ij}, y_{ij} | ϵ_{grid} | A few – a few 10 m | deg:min:sec | Multibeam | |
| Cell size | | | 100–200 m square | | GPS/DGPS | |
| Depth | $z_{i,j}$ | ϵ_d | A few 10 m | metre | | At centre beam |
| Internal clock*** | | | | | | |
| Deviation just before deploy | dt_3 | | $\sim 20 \mu\text{sec}$ | | | |
| Date of dt_3 | Date 3 | | | M:D:H:M:S | GPS clock | |
| Deviation just after retrieval | dt_4 | | $\sim 20 \mu\text{sec}$ | | | |
| Date 3 of dt_4 | Date 4 | | | M:D:H:M:S | GPS clock | |
| Duration | T_{duration} | | | days | | |
| Drift rate | $(dt_4 - dt_3)/T_{\text{duration}}$ | | $\sim 10\text{--}20$ msec/day | msec/day | | |

*Nichiyu Giken Kogyo Co. Ltd.

**Asada, A. personal communication.

***Tokyo Sokushin Co. Ltd.

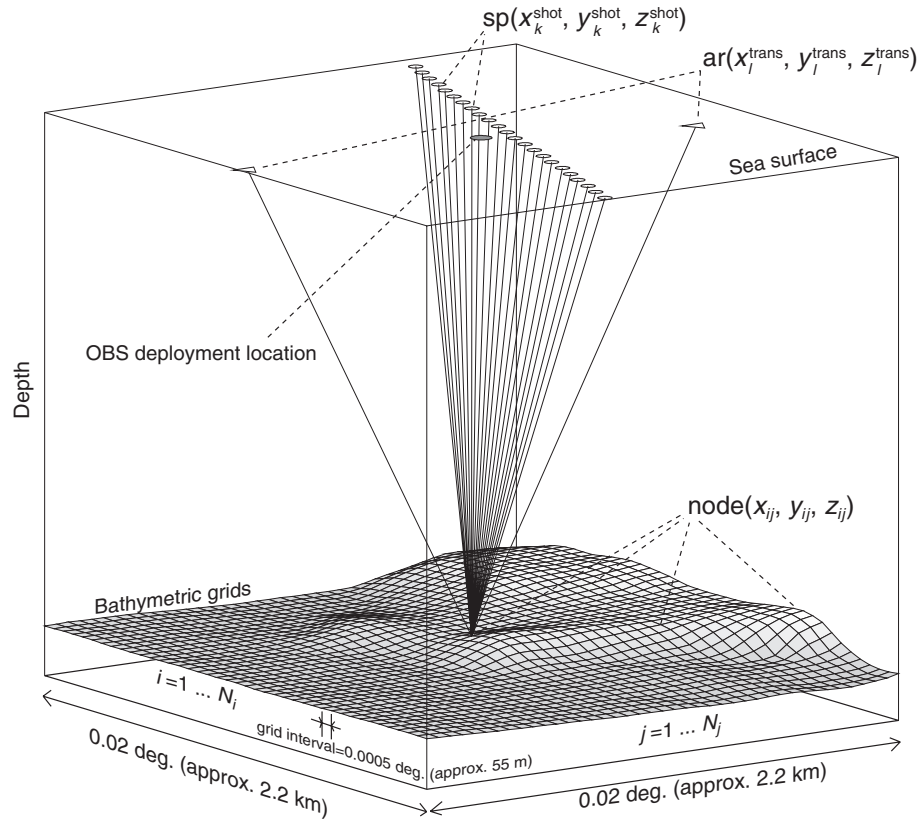


Fig. 2. Diagram showing spatial parameters using the global search method. sp: locations of the airgun shots; ar: locations of acoustic ranging by the transponders.

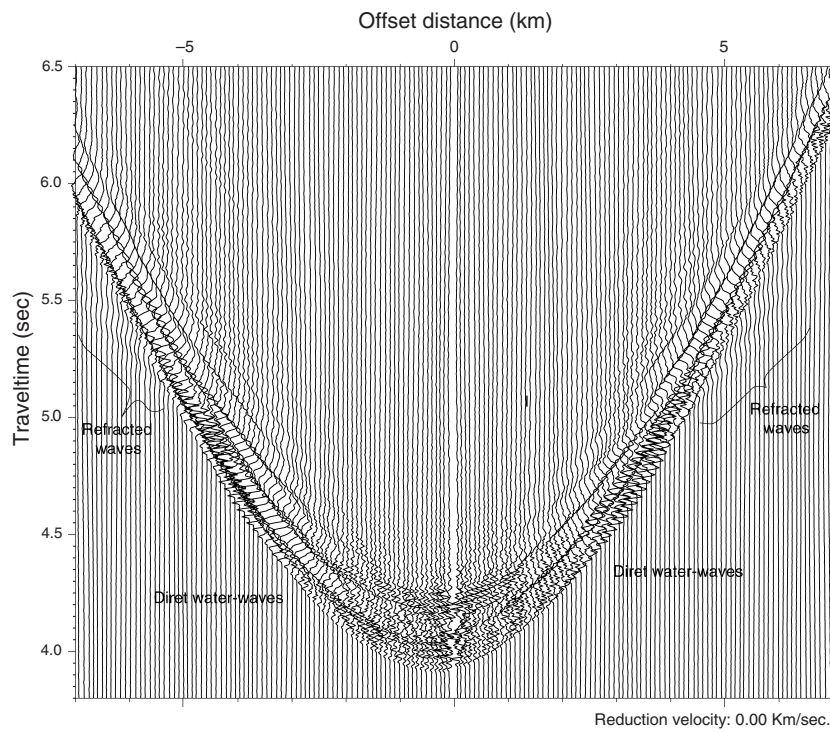


Fig. 3. An example for the observed hydrophone data recorded by an OBS. A shot interval is ~ 50 m. Refracted waves arrive earlier at distances greater than ~ 5 km. The fastest arrival of the direct water-wave appears at an offset distance of ~ -0.2 km because the temporary OBS location used to make the receiver gather was incorrect. Furthermore, larger trace intervals on records near 0 km offset distance suggest that the OBS was sited far off the airgun shot line.

search for the location of each OBS is 0.02×0.02 degrees ($\sim 2.2 \times 2.2$ km).

We need at least one dataset of airgun shooting passing over the OBS. If two datasets with different shooting dates and times are available, e.g. datasets for the seismic refraction and multi-channel seismic (MCS) reflection surveys, two different secondary correction terms for the OBS internal clock at the different times can be found by the non-linear inversion step of the new method. This secondary correction term of the OBS internal clock has not been considered in earlier papers (e.g. Shiobara et al., 1997). We use the data from the reflection survey for the global search step, because of the shorter airgun shooting intervals.

The acoustic transponder data are usually obtained as distances between the OBS and the acoustic transducer dangled from the side of the ship.

An average sound-speed of seawater, V_{mean} , is important for the global search and the non-linear inverse methods, especially when acoustic ranging data are available only at a single ship position. The average sound-speed of seawater is generally calculated by the standard equations (e.g. Del Grosso, 1974; MacKenzie, 1981) from XBT or XCTD data.

Global search method

The OBS can be located somewhere on the bathymetric grid nodes around the OBS deployment point. The direct water-wave traveltimes of the airgun shots $t_{\text{shot_obs}}(k)$ and the acoustic ranging traveltime data obtained by transponder system at one or two ship positions $t_{\text{trans_obs}}(l)$ are used in the method. More observations give better solution.

At first the following quantities are calculated to obtain two important global search parameters: the standard deviations of the airgun shooting traveltime residuals, and the root mean square of the acoustic transponder traveltime residuals, calculated from the distance measurements.

1) One-way traveltimes:

$$t_{\text{shot_cal}}(i, j, k) = \frac{\sqrt{(x_k^{\text{shot}} - x_{ij})^2 + (y_k^{\text{shot}} - y_{ij})^2 + (z_k^{\text{shot}} - z_{ij})^2}}{V_{\text{mean}}}, \quad (2)$$

where (x_{ij}, y_{ij}, z_{ij}) are node locations of the bathymetric grid data, and $(x_k^{\text{shot}}, y_k^{\text{shot}}, z_k^{\text{shot}})$ are the airgun shooting positions, respectively. k is an index of the airgun shot point; there are a total of N_k shot points.

We use the average sound-speed of seawater, V_{mean} , assuming a straight ray path between an OBS and an airgun shot point.

2) Differences between the observed and calculated direct water-wave traveltimes of the airgun shots:

$$\Delta t_{\text{shot}}(i, j, k) = t_{\text{shot_obs}}(k) - t_{\text{shot_cal}}(i, j, k). \quad (3)$$

There are significant variations in the Δt_{shot} values from node to node, as shown in Figure 4.

3) The average and standard deviation of Δt_{shot} , for every topographic node:

$$\overline{\Delta t_{\text{shot}}}(i, j) = \sum_{k=1}^{N_k} \Delta t_{\text{shot}}(i, j, k), \quad (4)$$

$$\sigma_{\text{shot}}(i, j) = \sqrt{\frac{1}{N_k - 1} \sum_{k=1}^{N_k} [\Delta t_{\text{shot}}(i, j, k) - \overline{\Delta t_{\text{shot}}}(i, j)]^2}. \quad (5)$$

If a node coincides with the true OBS location (Δt_{shot} is zero), the standard deviation $\sigma_{\text{shot}}(i, j)$ also takes a minimum value (ideally zero) at that node, under the assumption that parameters such as true V_{mean} , true bathymetric data, and true dt have been selected.

4) One-way traveltimes between a node and the acoustic transponder positions. This calculation uses transponder data and is done for every node of the bathymetric grid data as for equation (2):

$$t_{\text{trans_cal}}(i, j, l) = \frac{\sqrt{(x_l^{\text{trans}} - x_{ij})^2 + (y_l^{\text{trans}} - y_{ij})^2 + (z_l^{\text{trans}} - z_{ij})^2}}{V_{\text{mean}}}, \quad (6)$$

where $(x_l^{\text{trans}}, y_l^{\text{trans}}, z_l^{\text{trans}})$ is the position of the l -th acoustic ranging transducer. Here the traveltimes for acoustic ranging are calculated by distance measurements using the estimated average sound-speed of seawater V_{mean} .

5) Differences between the observed acoustic ranging one-way traveltimes and those calculated by equation (6), for every node of the bathymetric grid data:

$$\Delta t_{\text{trans}}(i, j, l) = t_{\text{trans_obs}}(l) - t_{\text{trans_cal}}(i, j, l). \quad (7)$$

The calculated traveltimes are based on error-free bathymetric data.

6) The root mean square (RMS) of the residuals from equation (7), for every bathymetric node:

$$RMS_{\text{trans}}(i, j) = \sqrt{\frac{1}{N_l} \sum_{l=1}^{N_l} [\Delta t_{\text{trans}}(i, j, l)]^2}, \quad (8)$$

where N_l is the total number of the acoustic ranging data.

Next, a bathymetric grid node is selected as an optimum OBS location, using σ_{shot} and RMS_{trans} calculated above. A 2D simulation result for σ_{shot} is shown in Figure 5a. An area with smaller values of σ_{shot} , including the OBS location, extends perpendicular to the airgun shot line in this figure. This shows that determination of the best OBS location in the direction parallel to the airgun shot line is easy, whereas it is not easy in the direction perpendicular to the line.

Figures 5b, 5c, and 5d show the 2D simulation results for RMS_{trans} , for three cases, with different numbers (1, 2, and 3) of acoustic ranging sites. A flat seafloor with a depth of 5000 m is assumed for all cases. The locations of the sites are shown by triangles in the inset maps. The acoustic ranging sites have been located 3 km away from the true OBS location, perpendicular to the airgun shot line, for 1 or 2 available sites (Figures 5b and 5c). Such acoustic ranging sites enable us to obtain areas of small RMS_{trans} , elongated perpendicular to the areas of small σ_{shot} , so giving a well defined intersection of RMS_{trans} and σ_{shot} . The intersection gives an optimum OBS location.

The OBS location resulting from this global search method is in practice given as the node location nearest to the intersection of the axes of the elongated areas of small σ_{shot} values (Figure 5a) and small RMS_{trans} values (Figures 5a, 5b, or 5c). Black dots in Figures 5a–5d indicate nodes on the axis of the area of small σ_{shot} . The node with the smallest RMS_{trans} value among the black nodes is chosen as the OBS location. Note that the OBS depth estimated here will be the seafloor depth given by the bathymetric grid data.

In the next step, the non-linear inverse method, the depth of the OBS, the average sound-speed of seawater, and the secondary correction term of the OBS internal clock are treated

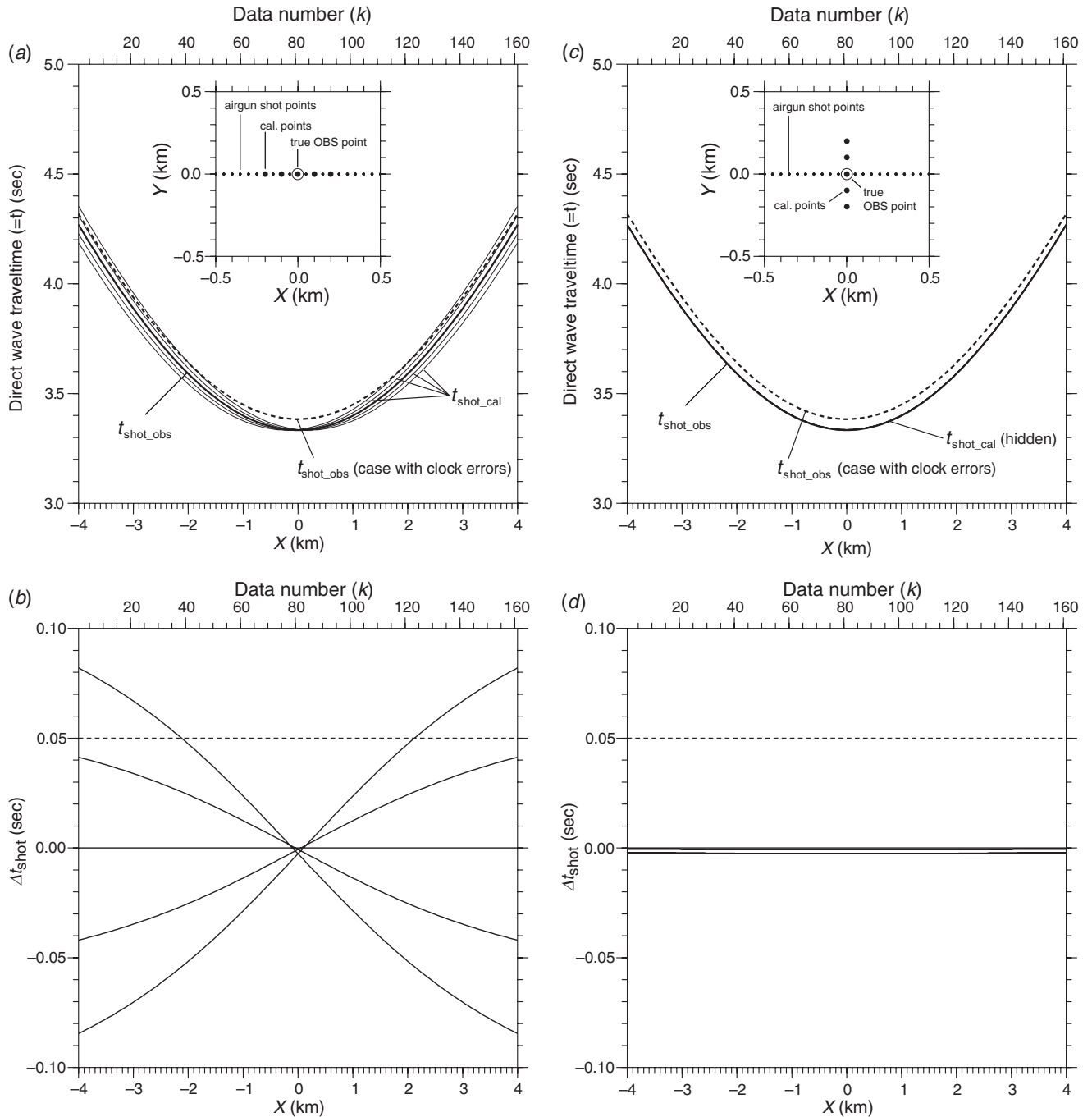


Fig. 4. Simulation of the direct water-wave from airgun shots, observed on the seafloor. A flat seafloor at a depth of 5000 m is assumed here. (a) and (b) are the calculated traveltimes and differences between observed and calculated times (O–C), when the locations used for calculations are shifted along the shooting line. The calculation points are located at –200, –100, 0, 100, and 200 m from the true OBS location in the *x* direction (along the shooting line). In this case, the Δt_{shot} value change is significant and it is easy to distinguish the true OBS site along the survey line. The broken line in (a) is the observed traveltime curve which includes an OBS internal clock error of 50 ms. In this case, the residual curve at the true OBS position becomes flat, with a constant value equivalent to the clock error (50 ms). (c) and (d) show the case where the trial OBS location is shifted perpendicular to the shooting line. In this case, the extent of Δt_{shot} change is small compared with the previous case, and it is not so easy to determine the true OBS location in the direction perpendicular to the shooting line.

as unknown parameters in addition to the horizontal location of the OBS. The values of these parameters will be slightly changed to minimise the differences between observed and calculated data.

Non-linear inverse method

The non-linear inverse method of Crosson (1976), for simultaneous least-squares estimation of hypocenter and

velocity parameters, is applied to improve the initial estimation of the OBS location found by the global search.

We assume that the airgun vessel traverses a line over the OBS in each direction, for the seismic refraction and reflection surveys. Two datasets of the direct water-wave traveltimes with two different dates and times can be obtained in this case. The secondary correction terms for the OBS internal clock are determined for both passes.

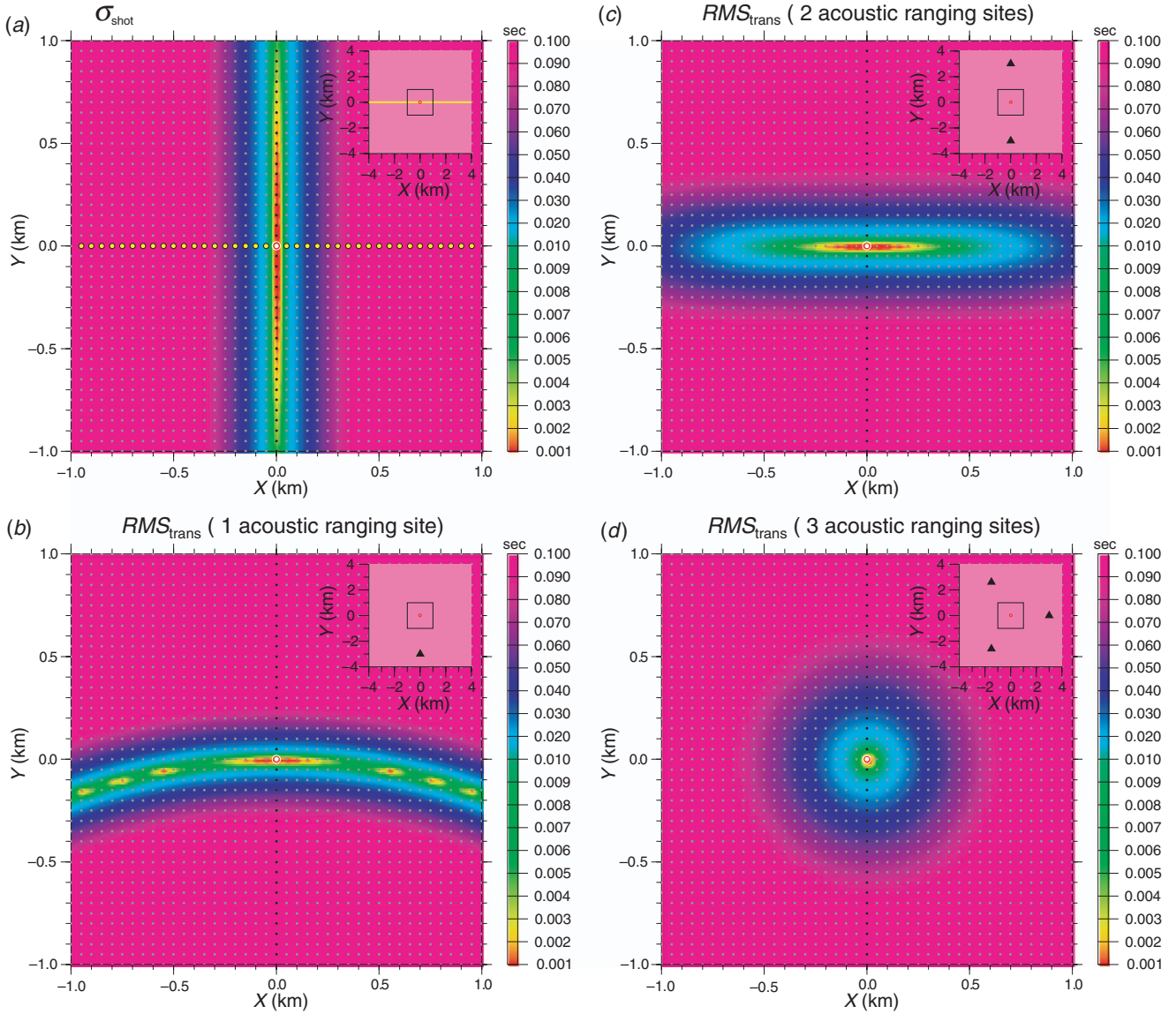


Fig. 5. 2D simulations of two important global search parameters: (a) the standard deviations σ_{shot} of the airgun traveltimes residuals, and (b–d) the RMS_{trans} of the acoustic transponder traveltimes residuals, calculated from the distance measurements for different acoustic ranging sites number of 1 to 3. (b) For one site, south of the shooting line. (c) For two sites, north and south of the shooting line. (d) For three sites surrounding the true OBS location. The locations of the acoustic ranging transceivers are indicated on the map inset in each figure. A flat seafloor with a depth of 5000 m is assumed in these simulations. The yellow dots in (a) show the airgun shot points. Red open circles in all figures indicate the OBS location. Black dots are optimum bathymetric node positions satisfying the airgun traveltimes data.

Assume that there are a total number of N observed traveltimes data $t_{\text{obs}}(i)$, including those of the airgun shots and of the acoustic transponder. A Taylor series expansion of $t_{\text{obs}}(i)$ in the neighbourhood of the traveltimes $t_{\text{cal}}(i)$ calculated by using the initial values $(x_0, y_0, z_0, v_w, t_{\text{clk1}_0}, t_{\text{clk2}_0})$ of the unknown parameters is as follows:

$$t_{\text{obs}}(i) - t_{\text{cal}}(i) = \frac{\partial t}{\partial x} \Delta x + \frac{\partial t}{\partial y} \Delta y + \frac{\partial t}{\partial z} \Delta z + \frac{\partial t}{\partial v_w} \Delta v_w + a_1 \Delta t_{\text{clk1}} + a_2 \Delta t_{\text{clk2}} + \varepsilon, \quad (9)$$

where (x, y, z) are coordinates of the location of the OBS, v_w is the unknown mean sound-speed of seawater, t_{clk1} and t_{clk2} are secondary correction terms of the OBS internal clock on the forward and reverse traverse over the OBS, respectively, and ε is an error term.

For the initial values (x_0, y_0, z_0) for the OBS location, we adopt the results of the global search method. Initial values t_{clk1_0} and t_{clk2_0} are 0 because the seismic record sections used for picking of the direct wave traveltimes have already been corrected for linear drift of the OBS internal clock. When the ship goes in one direction along the line, a_1 and a_2 take the values 1 and 0, respectively. When the ship goes in the reverse direction, a_1 and a_2 take 0 and 1, respectively. Furthermore, if $t_{\text{obs}}(i)$ is an acoustic transponder traveltimes, both a_1 and a_2 are 0 because the acoustic transponder traveltimes are not affected by the long-term drift of the OBS internal clock.

The six unknown quantities in equation (9) are of $(\Delta x, \Delta y, \Delta z, \Delta v_w, \Delta t_{\text{clk1}}, \Delta t_{\text{clk2}})$ so that we need seven or more observations of $t_{\text{obs}}(i)$ to apply a least-squares fitting method. The actual procedure of the non-linear inversion is described below.

To begin, the vector of residuals $\Delta \mathbf{t} = (\Delta t_1, \Delta t_2, \dots, \Delta t_N)^T$ and the solution vector $\Delta \mathbf{x} = (\Delta x, \Delta y, \Delta z, \Delta v_w, \Delta t_{\text{clk1}}, \Delta t_{\text{clk2}})^T$ are defined, where $\Delta t_i = t_{\text{obs}}(i) - t_{\text{cal}}(i)$. If \mathbf{A} is defined as the coefficient matrix whose elements are the partial derivatives of equation (9), the group of quasi-linear equations (9) can be written in a simple matrix notation:

$$\mathbf{A} \Delta \mathbf{x} = \Delta \mathbf{t}. \quad (10)$$

We use the Levenberg-Marquardt method, following Crosson (1976). Namely, we solve the following matrix

$$(\mathbf{A}^T \mathbf{A} + \theta^2 \mathbf{I}) \Delta \mathbf{x} = \mathbf{A}^T \Delta \mathbf{t}, \quad (11)$$

where \mathbf{I} is a unit vector and θ^2 is a weighting matrix. Finally we get the solution vector

$$\Delta \mathbf{x} = (\mathbf{A}^T \mathbf{A} + \theta^2 \mathbf{I})^{-1} \mathbf{A}^T \Delta \mathbf{t}. \quad (12)$$

This procedure is iterated until convergence criteria are met.

The unknown parameter changes should be small because good initial values obtained by the global search method are used. If the values of the unknown parameter are significantly changed from the initial values, or the final root mean square of differences between the observed and calculated values is large (about greater than 10 ms), the input data should be checked again.

Case study

In this example, the ocean bottom slopes steeply, and the depth varies from 5250 m to 4600 m in the search area (Figures 6c and 6d). The calculated standard deviations σ_{shot} using airgun direct water-waves are shown in Figure 6a. It can be seen that low σ_{shot} values are distributed nearly perpendicular to the survey line (shown by yellow dots). Black dots are nodes located on the axis of the low σ_{shot} zone. These nodes are candidates for the possible OBS location.

In the next, we determine the best node using RMS_{trans} (Figure 6b). The position of transponder used is located at 3.7 km SE of the OBS deployed location. The low RMS_{trans} zone is nearly perpendicular to the black dots zone. We chose the global search OBS position (open red circle) to be the node at the intersection of the axes of the low RMS_{trans} zone and black dots zone. The yellow lines in Figures 6b, 6c, and 6d show $\Delta t_{\text{trans}} = 0$ contours based on the traveltimes obtained by the transponder and the depths given by bathymetric grid data. Ten lines overlap in the figure, because the ranging data were observed at only one location, so the values are almost the same. The OBS position obtained by the global search is determined to be the location shown by a red open circle, 250 m away from the deployed position. The reliability of the transponder measurements for this example was independently examined.

Figures 6c and 6d shows the results of the global search and non-linear inversion methods, shown by the red open circle and red open star over the bathymetry, respectively. The result of the non-linear inversion using the start position obtained by the global search (red open star) is only 24 m (horizontal) and 0 m (vertical) from the global search result (red open circle), and is consistent with topography. On the other, applying non-linear inversion with the OBS deployment location and corresponding depth as initial values results in an OBS depth (4 811 m) inconsistent with topography (5 110 m). If the ocean bottom topography is gentler or flat, the two results would be almost the same in horizontal location and depth. The vertical misplacement of the OBS location gives rise to bigger errors in crustal structure studies (especially in 2D modelling) than horizontal misplacements. However, if transponder data

measured at more than three appropriate positions are available, and the OBS location as initial values for non-linear inversion can be estimated by using these data, the difference between the global search and non-linear inversion results will be smaller. In other words, the global search step is more effective where there are few acoustic transponder data (<3 sites).

Figure 6e shows the observed direct water-wave traveltimes $t_{\text{shot_obs}}$ of the airgun shots and calculated traveltimes $t_{\text{shot_cal}}$ at the node which is selected as the most probably location of the OBS by the global search method (shown by red open circles in Figures 6a–6d). The differences between the $t_{\text{shot_obs}}$ and $t_{\text{shot_cal}}$ ($= \Delta t_{\text{shot}}$) are shown in Figure 6f. An average of the Δt_{shot} (–10 ms for this case) gives the secondary correction term for the OBS internal clock. Although Figures 6e and 6f use the result of the global search, there is no significant difference between the final result after the non-linear inversion and this result.

Figures 6c and 6d show $\Delta t_{\text{shot}} = 0$ contours (white lines) for each airgun shot before and after applying the secondary correction term for the OBS internal clock, indicated by Figure 6f. An intersection of the white lines gives the optimum OBS location. There is no significant difference between Figures 6c and 6d, because of the small secondary correction term for the OBS internal clock. If the secondary correction term for a specific OBS is large (perhaps a few tens of milliseconds) compared with the possible overall errors, the seismic record section should be edited by using the OBS internal clock time taking into account both the secondary correction term and the ordinary time correction. The secondary correction terms of most of the OBSs that we have treated were not so large that the results of the crustal structure study were changed. Nevertheless, some OBSs have shown severe time drifts. We can use such OBSs by applying the secondary corrections.

In this case study, the RMS of the direct water-wave traveltime residuals is 4 ms and the standard deviation of the solutions is 8 m, 8 m, 4 m, 2 ms and 2 m/s for latitude, longitude, depth, the secondary time correction term, and the sound-speed of seawater, respectively.

Discussion

Although in the example above we did not include the measurement errors in the dataset that we used, the actual data might have some measurements errors that might cause location errors. Here, we examine the influence of measurement errors associated with the parameters used in the calculation. The measurement error in each parameter is listed in Table 1. We discuss the effect of each of these errors in turn.

Errors associated with airgun shooting

The shot times of airgun shots $t_0(k)$ are based on a GPS clock, with errors less than 10 μs . The ship positions during shots, $(x_k^{\text{shot}}, y_k^{\text{shot}})$, are usually determined by DGPS fixing with a position error of less than a few metres. The position differences between the airgun array towed behind the ship and the DGPS fix are corrected for. This means that the errors in airgun shot position and time are insignificant compared with the errors in bathymetric data, acoustic ranging data, average sound-speed of seawater, and probably the internal clock of OBSs.

Traveltime errors for airgun shooting

The reading errors of direct water-waves, $\varepsilon_{\text{pick}}$, are normally less than 10 ms, including ± 2.5 ms digitisation uncertainty if the sampling rate is 200 Hz, and the time delay due to band-pass filter (5–30 Hz) is small. The effect on travel times of refraction of the direct water-wave ray path is as small as a few milliseconds.

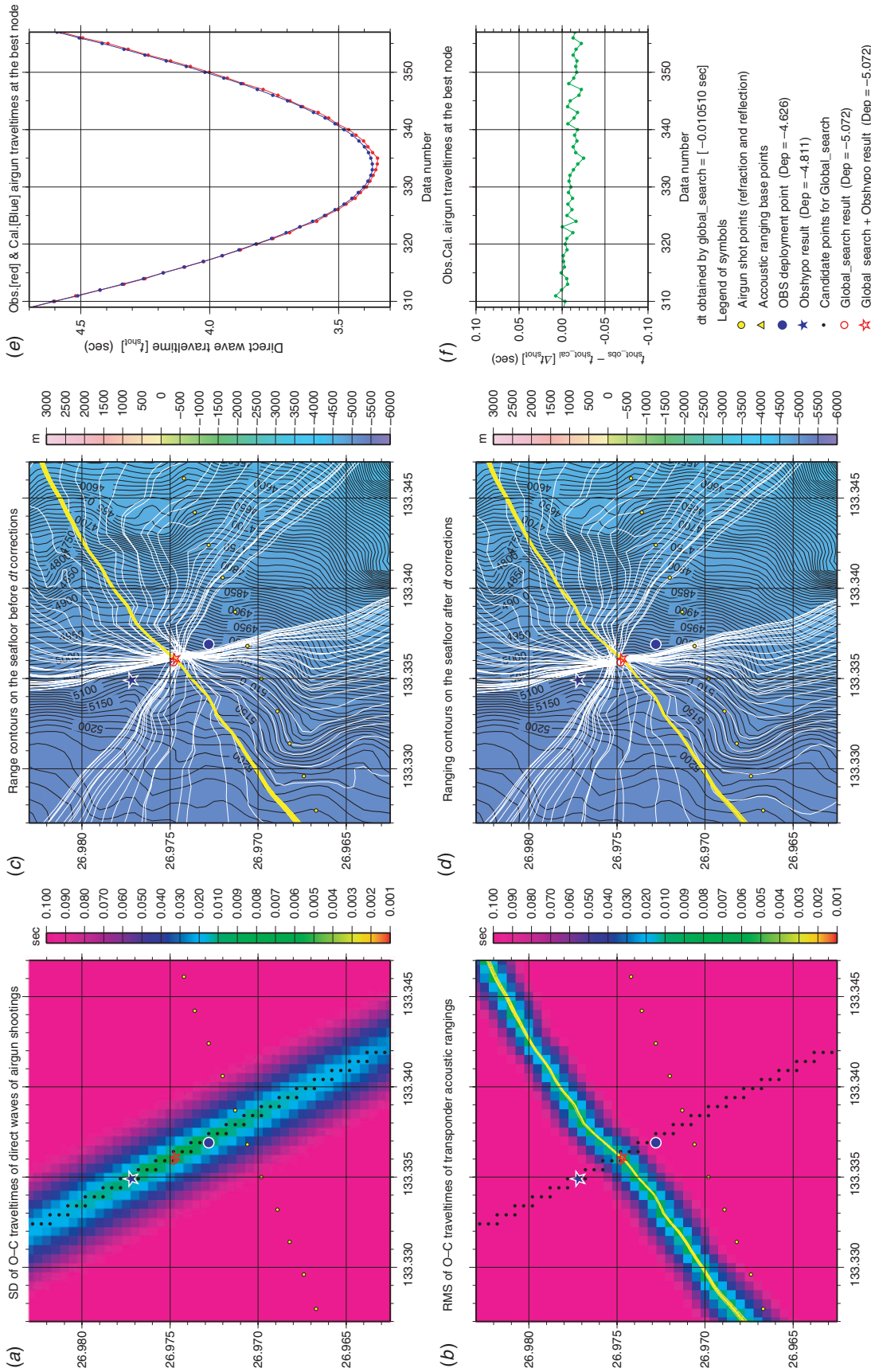


Fig. 6. Case study of OBS locating using the global search and non-linear inversion methods. The symbol legend is at the bottom right. (a) Standard deviations σ_{shot} of differences between observed and calculated traveltimes (O-C) of the direct water-waves from airgun shots. The shot locations are shown by yellow dots. Black dots are optimum bathymetric positions satisfying the airgun traveltimes data. (b) Root mean squares (RMS_{trans}) of traveltimes residuals obtained from acoustic ranging. The yellow line is a contour line drawn on the seafloor satisfying the traveltimes for each measurement. A transponder is located at 3.7 km SE of the true OBS location. (c) and (d) Contour line (white) drawn on the seafloor satisfying the traveltimes for each airgun shot obtained, (c) without the second stage time correction and, (d) with the second stage time correction. Note that by applying the second stage time correction to the OBS internal clock, the sum of differences between the observed and calculated traveltimes of whole airgun shots becomes a minimum at the final OBS location. (e) Observed (red dots with line) and calculated (blue dots with line) traveltimes curves for the best node determined by the global search method using the precise bathymetric grid data, the airgun shot times, the first stage time corrections, and the average sound-speed of seawater. Although the shapes of the both curves are similar, slight parallel shifts in traveltimes and horizontal axes directions are present. (f) Traveltimes residuals, for data shown in (e). Due to determination errors and the finite spacing of bathymetric grid nodes, the residual curve has some trend.

Bathymetric grid data

If the bathymetric data have some measurements errors, the estimated Δt_{trans} may cause some grid search error in the global search method. The absolute errors associated with bathymetric data are not well known. They depend on grid sizes, seawater sound-speed used, ship positions during the survey, signal-to-noise ratios due to the sea-state during the bathymetric survey, and beam-pin locations. The location error of the survey vessel during the bathymetric survey may be a few ten metres if the survey vessel used the ordinary GPS navigation (error: $\varepsilon_{\text{grid}}$). In an average survey situation, the precision of bathymetry (error: ε_d) is roughly of the order of a few tens of metres (0.5% of water depth) for the centre beams of a multi-beam echo sounder (Monahan and Wells, 2000; Asada, A., personal communication). Although a secondary time correction term is obtained in the non-linear inversion step, we do not know the true cause of the apparent secondary time correction term. Bathymetric error may be partly responsible. If the sea-bottom is extremely rough, there may occur deviations from the normal hyperbola that cause misidentification of the appropriate grid node.

Internal clock accuracy

The OBS internal clock should have better accuracy than 10^{-7} . Nakamura et al. (1987) suggested that the time correction for the internal clock drift is less than a few milliseconds. The secondary correction term for the internal clock may not be so large (~ 10 – 20 ms) if we use a clock with precision $< 10^{-7}$, although the time span for the time corrections is rather longer than that of the airgun shots. In our experience, the additional time correction is only necessary for a very few OBSs, unless the temperature correction terms for the OBS clock is incorrectly adjusted. Although most of the internal clocks show < 20 ms/day drift rates, there are some exceptional cases showing extremely large drift rates, more than 100 ms/day. Such internal clocks may not be fully corrected by the $dt(k)$ values of equation (1), and this is the reason why we calculate the secondary correction term for the internal clock.

Transponder measurements

The ship positions for transponder measurements, $(x_i^{\text{trans}}, y_i^{\text{trans}})$, can be measured with a few tens of metres error if the ship uses ordinary GPS methods (error: $\varepsilon_{\text{ship_pos}}$). The horizontal distance between the GPS antenna and the acoustic transducer, and the depth at which the acoustic transducer is deployed, should also be corrected for, to reduce uncertainty. The distance data are divided by the sound-speed of seawater to get the traveltimes between the OBS and the observation points. The transponder error might contribute 100–150 m uncertainty for the final OBS position calculated by this algorithm.

Sound-speed errors

The sound-speed of seawater can range from 1470 to 1540 m/s, and the estimation error, ε_v , is 70 m/s for the worst case. This corresponds to 46 ms in water wave travel time. We may use more reliable average sound speeds if there are some CTD, XCTD, or XBT measurements. In this case, the estimation error, ε_v , may be < 10 m/s which corresponds to < 7 ms.

Overall determination errors

Nodes on the axis of the elongated area of σ_{shot} values are shown by black dots in Figure 5. For example, if we consider ~ 20 ms for the internal clock error, ~ 20 ms ($= \sim 30$ m/1500 m/s) for bathymetric data error, ~ 26 ms (water depth: ~ 6000 m; sound

speed 1500–1510 m/s) for sound-speed estimation error and ~ 10 ms for reading error, the possible total error comes to ~ 76 ms which is equivalent to more than 1 km from the estimated OBS position seen in Figure 5a. If we use only airgun traveltimes, it is difficult to choose the best OBS location. This suggests that the transponder data are extremely important to find the true OBS position.

In the example shown in Figure 6, the time differences between the observed traveltimes $t_{\text{shot_obs}}$ including reading errors and the calculated traveltimes $t_{\text{shot_cal}}$ are ~ 10 ms (Figure 6f). Although this is a common result, we know from experience that OBSs showing larger $t_{\text{shot_cal}}$ residuals may occur. If a 50 ms residual is caused by depth errors, it implies an error of ~ 75 m, which seems large (Monahan and Wells, 2000; Asada, A., personal communication). If a 50 ms residual is due to errors in the sound-speed of seawater, the corresponding error would be ~ 20 m/s, which is also too large. It seems that a combination of depth error, sound-speed error of seawater, airgun arrival picking errors and clock correction error would all contribute to an apparent secondary time correction of 50 ms. The non-linear inversion calculates the final OBS position and the secondary time correction term. Because we cannot evaluate true measurement error in an actual case, the secondary time correction might be the resultant of all individual measurement errors, and we use this secondary time correction term in actual crustal structure studies.

In the first part of the global search method, the results define a narrow zone nearly perpendicular to the shot line. The width of this narrow zone is approximately the shot spacing, as large as 50 m, because we cannot determine the location of travel time minima between two adjacent shot locations. The second part of the global search uses the transponder distance measurements. If the zero traveltime residual lines (yellow lines in Figures 6b–6d), or the axis line of RMS_{trans} (Figure 6b), given by the transponder location are nearly perpendicular to the zone given by the first part, the error due to this part is as large as errors in the ship navigation fixes. In an extreme case, they might be ± 100 – 150 m. This may not cause serious problems, because the additional time change due to horizontal offsets perpendicular to the shooting line is less than 10 ms. However, if the transponder data are really erroneous, the location error will be very large.

The RMS of traveltime data residuals in the case study described above is 4 ms. In our experience, the values of the RMS of residuals have been around or smaller than 10 ms, if significant observation errors have not included in the data. Thus, we infer that the OBS position can be estimated by our positioning method with an accuracy of a few tens of metres.

Conclusions

In crustal structure studies in oceanic regions, OBSs and airguns are powerful tools. The OBS positions are one of the key parameters in crustal structure studies. To determine these key parameters as well as possible, we have developed a new method determining OBS positions using airgun shots and bathymetric data in addition to distance measurements using acoustic transponders. The new method can determine OBS positions using precise bathymetric grid data and direct water-wave traveltimes of airgun shots, together with acoustic ranging traveltimes measured at only one or two sites. A global search method gives the OBS location as initial values for a non-linear inversion method. Using an OBS location from the global search step, the non-linear inversion can determine the final OBS location properly without falling into traps of local convergence minima. The new method can also obtain a secondary correction

term for the OBS internal clock, but we consider that this correction term also includes the effects of other kinds of error. For both the global search and the non-linear inversion methods, it is also important to give proper initial values for the average sound-speed of seawater.

We have evaluated the influence of the error associated with each dataset. Although it is believed that the internal clock in the OBS, being more accurate than 10^{-7} , may not have a large influence on the final position errors, it is necessary to make secondary clock corrections for some OBS clocks. The second correction term is determined by the non-linear inversion in our method. Other parameters, such as bathymetric grid data and the average sound-speed of seawater might also have some error, and the secondary time correction might be resultant of errors in the OBS internal clock, the bathymetric data, and the average sound-speed of seawater. Where an OBS shows large daily drifts of its internal clock, the secondary time correction should be applied. Errors related with the acoustic ranging using the transponder system may cause ~ 100 – 150 m horizontal offset from the best OBS position, but these may not give rise to severe problems in crustal structure studies because the additional time change due to horizontal offsets perpendicular to the shooting line is less than 10 ms.

Acknowledgments

We give our thanks to the staff of Japan Continental Survey Co. Ltd., Kawasaki Geological Engineering Co. Ltd., and JGI Inc. We particularly thank Dr. Kayoko Tsuruga, Mr Shigeharu Mizohata and Mr Yasuo Tamura for their valuable comments during this study. The authors are also grateful to two anonymous reviewers for their valuable comments. Most of the figures in this paper were prepared using the GMT graphics package of Wessel and Smith (1998).

References

- Crosson, R. S., 1976, Crustal structure modeling of earthquake data. 1. Simultaneous least squares estimation of hypocenter and velocity parameters: *Journal of Geophysical Research* **81**, 3036–3046.
- Del Grosso, V. A., 1974, New equation for the speed of sound in natural waters (with comparisons to other equations): *Journal of the Acoustical Society of America* **56**, 1084–1091. doi: 10.1121/1.1903388
- Kasahara, J., Kubota, R., Tanaka, T., Mizohata, S., Nishiyama, E., Nishizawa, A., and Kaneda, K., 2007, New precise method for the crustal structure analysis using OBS and control sources: *Japan Geoscience Union Meeting 2007, JGU, Abstract*, O135–007.
- MacKenzie, K. V., 1981, Nine-term equation for the sound speed in the oceans: *Journal of the Acoustical Society of America* **70**, 807–812. doi: 10.1121/1.386920
- Monahan, D., and Wells, E., 2000, IHO SP 44 standards for hydrographic surveys and the demands of the new century: *Proceedings of Canadian Hydrographic Conference*, Montreal, Quebec, 15–19 May, CD-ROM.
- Nakamura, Y., Donoho, P. L., Roper, P. H., and McPherson, P. M., 1987, Large-offset seismic surveying using ocean-bottom seismographs and air guns: instrumentation and field technique: *Geophysics* **52**, 1601–1611. doi: 10.1190/1.1442277
- Shiobara, H., Nakanishi, A., Mjelde, R., Kanazawa, T., Berg, E. W., and Shimamura, H., 1997, Precise positioning of ocean bottom seismometer by using acoustic transponder and CTD: *Marine Geophysical Researches* **19**, 199–209. doi: 10.1023/A:1004246012551
- Wessel, P., and Smith, W. H. F., 1998, New, improved version of the generic mapping tools released: *EOS Transaction of American Geophysical Union* **79**, 579. doi: 10.1029/98EO00426

Manuscript received 11 September 2007; manuscript accepted 28 November 2007.

エアガン発震と精密水深データを使った地殻構造解析のための 新しい海底地震計位置決定方法

押田 淳¹・久保田隆二¹・西山英一郎¹・安藤 潤¹・笠原順三²・西澤あずさ³・金田 謙太郎³

要 旨: 海底地震計 (以下, OBS と呼ぶ) の位置は, OBS とエアガンを使った地殻構造解析における重要な要素のひとつである。通常, OBS の位置決定には, 音響トランスポンダによる測距を 3ヶ所以上で実施する必要がある。しかし, 時間的制約などの理由により, 観測点数を減ずる場合も多い。我々は, この様な数量的に十分でない音響トランスポンダによる測距データに加えて, OBS に記録されたエアガン発震による水中直達波と精密水深データを使用した OBS の新しい位置決定方法を開発した。この新しい方法は 2つのステップで構成される。その第 1 ステップでは音響トランスポンダによる測距データとエアガン発震の水中直達波の走時を最もよく説明できる OBS 着底位置を, OBS 投入位置周辺の水深グリッドデータのノードの中から探索する (小論ではグローバルサーチと呼ぶ)。精密水深データの使用は, OBS 着底位置近傍の海底地形が急峻な場合には特に重要となる。第 2 ステップでは非線形インバース法が実施され, 最終的な OBS 着底位置を決定する。その際に, 第 1 ステップで得られた水深グリッドデータのノード位置を初期値として用いることで, 求める解が局所的最小値に収束してしまうことを防止している。本手法では, OBS の最終位置に加えて OBS 内部時計の 2次補正項も得られる。OBS 位置の決定に使用した各測定値の誤差と結果に与える影響についても議論した。

キーワード: 海底地震計, 地殻構造, OBS 位置, エアガン, 水深グリッドデータ, 音響トランスポンダ

지각구조 연구에서 에어건 발파와 정밀 수심 자료를 이용한 OBS 위치 결정의 새로운 방법

Atsushi Oshida¹, Ryuji Kubota¹, Eiichiro Nishiyama¹, Jun Ando¹, Junzo Kasahara², Azusa Nishizawa³, and Kentaro Kaneda³

요 약: 지각구조 연구에서 해저면 지진계(OBS)의 위치정보는 OBS-에어건 탄성과 탐사에 있어서 매우 중요한 변수들중의 하나이다. 이 변수의 정확도를 향상시키기 위해 우리는 이용 가능한 음향 트랜스폰더에 의한 거리 정보와 함께 에어건 발파 자료와 수심 자료를 이용하여 OBS 위치를 결정하는 새로운 방법을 개발하였다. 음향 트랜스폰더로 얻은 거리 자료가 3 지점 미만의 것일 때에는 에어건 발파에 의해 발생하여 OBS에 기록된 수중 직접파의 주기가 OBS 위치 결정에 매우 중요한 정보로 활용된다. 그 새로운 방법은 두 단계로 이루어져 있다. 첫 번째 단계에서는 광역 검색이 이루어지는데 이는 수심 격자상에서 에어건 발파로부터 나온 수중 직접파의 관측 주기와 트랜스폰더 시스템을 사용하여 얻은 음향 거리로 설명할 수 있는 가장 가까운 노드를 찾는 것이다. 만약 OBS가 위치한 해저면 지형이 매우 험하다면 정밀한 2D 수심 데이터의 사용이 가장 중요하다. 국부적으로 수렴하는 최소값에 빠지지 않기 위해 첫 번째 단계에서 얻은 노드의 위치는 두 번째 단계의 초기값으로 사용된다. 두 번째 단계에서는 비선형 역산법이 수행된다. 만일 OBS의 내부 시계가 큰 편차를 보인다면 이 방법을 사용한 최종 OBS 위치와 함께 내부 시계에 대한 보정 또한 이루어져야 한다. 우리는 여기에서 OBS 위치 결정에 사용한 각 측정값의 영향과 오차에 대해서도 토론하고자 한다.

주요어: 해저면 지진계(OBS), 지각구조, 해저면 지진계 위치, 에어건, 수심 격자 자료, 음향 트랜스폰더

1 川崎地質 (株)
〒108-8337 東京都港区三田 2-11-15
2 日本大陸棚調査 (株)
3 海上保安庁 海洋情報部

1 카와사키 지질 (주)
2 일본 대륙봉조사 (주)
3 해상보안청, 해양정보부